RSC Advances

ROYAL SOCIETY OF CHEMISTRY

www.rsc.org/advances

RSC Advances

RSCPublishing

PAPER

Hydrophilic Pore-Blocked Metal-Organic Frameworks: A Simple Route to Highly Selective CH_4/N_2 Separation.

Cite this: DOI: 10.1039/x0xx00000x

Received 00th January 2012,
Accepted 00th January 2012

DOI: 10.1039/x0xx00000x

www.rsc.org/

Daeok Kim and Huen Lee*

Separation of gas mixtures with similar thermodynamic and transport properties is challenging issue. For that, various types of adsorbents and membranes have been introduced. Until now, solving this difficult problem remains an urgent core task in the energy and environment fields. Herein, we introduce the simple method to achieve highly selective separation of CH_4/N_2. To demonstrate our concept, a CH_4/N_2 mixture was separated by Cu_3BTC_2 filled with water, with the water blocking the hydrophilic pore to reject the inclusion of gas molecules having weak affinity for water, with empty hydrophobic pores acting as gas storage sites. This led to high equilibrium selectivity of the CH_4/N_2 mixture, at 24.7, which is 6 times higher than untreated Cu_3BTC_2 itself. Also, formation of methane hydrate in the mesopore of MOF was observed.

Broader context

Natural gas is a fossil fuel of growing importance due to its abundance in various forms, environmental friendliness and availability of large reserves. To meet the global energy demands, production and consumption of natural gas are rapidly increasing. This circumstance has been accelerating the use of both low quality and unconventional natural gas such as shale gas, coal bed methane, tight gas and methane hydrate, etc. which contain considerable amount of impurities. For the actual use in industry, impurities such as H_2S, CO_2, N_2 should be separated. Especially development of efficient CH_4/N_2 separation technology has been one of the important issues in natural gas industry. The similar physical properties of CH_4 and N_2 make the separation difficult. For the reason, cryogenic distillation consuming huge amount of energy has been practically used in large scale. For economic removing of N_2, arising technologies based on pores such as membrane, nanoporous materials including molecular gate technology using pressure swing adsorption have been introduced to replace conventional method. To enhance the performance of those technologies, low CH_4/N_2 selectivity remains to be overcome. Here, we demonstrated that blocking the hydrophilic pore of porous material composed of both hydrophilic and hydrophobic pores can lead to the extremely high CH_4/N_2 selectivity. This new approach can lead to further development of highly selective adsorbents and membranes.

Introduction

Pores, confined space which allow molecular passage and which facilitate occupation, are meaningful structures in various science disciplines. They are observed in various systems ranging from cell membrane to rocks. Materials incorporating pores are called porous materials, and these have provided unprecedented opportunities to develop emerging technologies such as catalysts, fuel cells, ion exchange mechanisms, molecular storage systems and separation mechanisms. In particular, porous materials reveal tremendous potential in the field of molecular separation in relation to the synthesis of new porous structures. They also offer technological advances when seeking to manipulate pore properties such as the pore size, size distribution, shape and surface functionality. Membranes, porous materials which are receiving much attention at present, separate molecular mixtures based on the difference in the permeability of molecules through incorporated pores, are expected to provide energy-efficient processes in industry. Such methods have been successfully applied in industrial areas such as hydrogen recovery (from H_2/N_2, H_2/CO_2, and H_2/CH_4), air separation (N_2/O_2), and CO_2 separation (from CH_4, CO, N_2 or hydrocarbons).[1-5] Microporous materials such as zeolites and metal organic frameworks also show notable performance levels when used in gas separation applications. The separation process is induced by the difference in the interaction between the gases with functionality incorporated in the materials. Recently, Long et al. reported the successful separation of olefin-paraffin mixtures having similar molecular sizes and volatility levels using an MOF with open iron(II) coordination sites[6] as well as hexane isomers using an MOF with triangular channels.[7] Regarding the separation of gas mixtures, the introduction of functionalities such as open metal sites[8,9] a functional group attached to a linker[10,11] and a target-designed cavity known as a 'single molecular trap'[12,13] in porous material leads to high selectivity for CO_2.

Graduate School of EEWS and Department of Chemical & Biomolecular Engineering (BK-21 plus), Korea Advanced Institute of Science and Technology, 291 Daehak-ro, Yuseong-gu, Daejeon 305-701, Republic of Korea *E-mail:H_lee@kaist.ac.kr*

†Electronic Supplementary Information (ESI) available. See DOI: 10.1039/b000000x/

Despite the bright advances and good results in gas separation using porous materials, realizing the separation of gas mixtures having similar physical and transport properties is not easy task. Their low separation efficiency remains a difficult and urgent issue.

We note that there are two possible routes to overcome the current limits and achieve a highly selective molecular capturing process. The first route would be to design and synthesize new porous materials via chemical modification, as considerably demonstrated by a number of porous materials. The second route would be to use the physical nature of diverse gas storage compounds, favorably offering facile scale-up capabilities and good cost-effectiveness. We tried enhancing the affinity between target molecules and a surface or confined space dramatically via the second route to facilitate highly selective gas separation.

Here, we introduce a simple physical treatment of nanoporous materials composed of both hydrophilic and hydrophobic pores to invoke a highly selective gas capture and rejection mechanism. The insertion of hydrophilic molecules causes the hydrophilic pores to be occupied while the hydrophobic pores remain empty and store hydrophobic molecules, and vice versa. This is achieved spontaneously by instigating contact between an inserted molecule and appropriate porous materials. The inserted molecules change the pore structure and properties, thus tuning the affinity for specific gases within the pore networks.

Experimental Section

Cu_3BTC_2 was synthesized by slightly modifying a previously reported solvothermal method.[14] Copper nitrate trihydarte (4.35 g, Sigma Aldrich) and trimesic acid (2.1 g, Sigma Aldrich) were dissolved in solvent that consists of ethanol (60 ml, Junsei Chemical Co.) and deionized water (60 ml). As prepared solution was mixed for 12 hours and sonicated for 30 min then placed in stainless reactor and went through reaction at 120 ℃ for 12 hours. As synthesized crystalline solid was washed with ethanol 3 times a day for 2 days then dried at room T for 12 hours and at 180 ℃ for 12 hours. To prepare HPB-Cu_3BTC_2, dehydrated Cu_3BTC_2 was placed in a vacuum oven with a beaker containing water and evacuated to 4 torr, where the relative humidity was 100 %. HPB-Cu_3BTC_2 (1.5 g) was loaded into a high-pressure cell (6 mL), pressurized at room temperature and then kept at -30 ℃ for 1 day. To measure its storage capacity the pressurized cell was vented at -30 ℃ and kept at room temperature to dissociate stored gas. The volume of gas emitted was measured by the water displacement method described in Fig. S1†. The CH_4/N_2 gas, purchased from (Special gas, Korea), was pressurized at -30 ℃ for separation. The dissociated gas was injected into a GC equipped with a TCD sensor as described in Fig. S2†. The LT-XRD, HPRD, Raman and NMR analyses were done after precooling the reactor with liquid nitrogen. The samples were finely ground to particles smaller than 200 um at 77 K, and placed in a pre-cooled sample loader. Diffraction was performed by: 1) Low Temperature XRD (D/MAX, Rigaku) with CuK radiation (λ=1.5406 Å) at a generator voltage of 40 kV and generator current of 300 mA, and 2) HRPD using the synchrotron at the Pohang Accelerator Laboratory (λ = 1.54950 Å). A Raman analysis was performed using a high-resolution dispersive Raman microscope (Horiba Jobin Yvon LabRAM HR UV/Vis/NIR) with 514.53 nm light emitted from an Ar-ion laser (30 mW) at -180 ℃ with the following measurement conditions: 1800 grating, D1 filter and 1000 hole. All the Raman measurements were performed with Cu_3BTC_2 single crystal as shown in Fig. S3†. The sample pressurized with 13C CH_4 was analyzed with a 400 MHz 13C CP-MAS Solid NMR (BRUKER) at 4 K spinning rate and at -40 ℃.

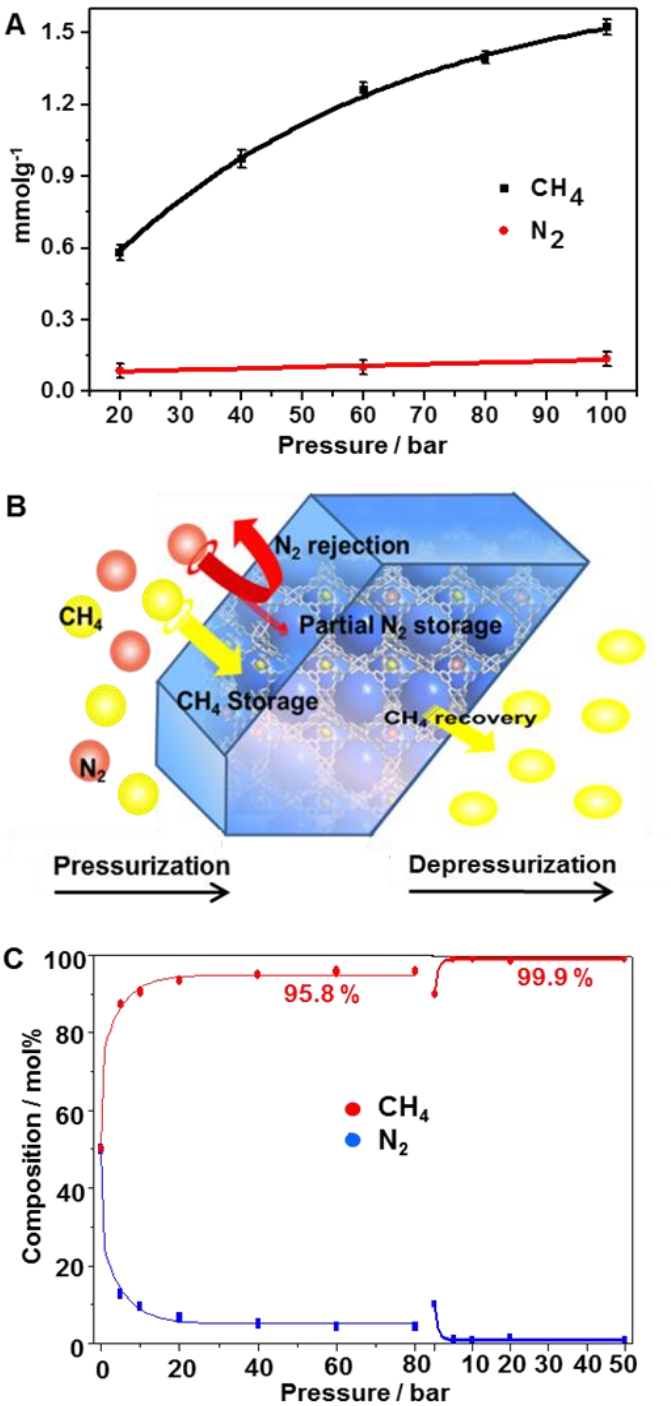

Fig. 1 Gas storage and separation of HPB-Cu_3BTC_2. (A) The stored amount of CH_4 (black) and N_2 (red) in relation to pressure. The line is fitted from experimental data. Each point is average value after 3 times measurement and the error bars indicate standard deviation within (± 0.03). (B) Schematic description of gas separation mechanism in HPB-Cu_3BTC_2. (C) Composition of stored gases after exposure to equimolar (left) and 90/10 (right) mixtures of CH_4/N_2 at various pressures.

Results and Discussions

To demonstrate our concept and its effectiveness and simplicity, we undertook the separation of CH_4/N_2 mixtures. Thus far, CH_4/N_2 separation has mainly been done by means of cryogenic distillation, which requires considerable amounts of energy to cool the CH_4. To overcome the technical and economic barriers of energy and cost aspects, versatile separation technologies based on absorption, adsorption, and membranes were extensively adopted,[3] however, the poor specific gas selectivity associated with these methods sets strict limits on their practical use. Under these circumstances, we adopted our approach to the Cu_3BTC_2 (BTC: 1, 3, 5–benzentricarboxylate) metal organic framework (MOF), by which the 'hydrophilic pores are blocked' (HPB) with water molecules and the hydrophobic pores are empty. The material was chosen because it is one of the most characterized MOFs, showed maintenance of porous structure in our working condition, and contains both hydrophilic and hydrophobic pores together. In addition it is already commercially available.

Cu_3BTC_2 contains three types of pores 5, 10.6 and 12.4 Å of pore size, respectively.[15] The smallest pore is surrounded by four benzene rings and exhibits hydrophobicity. The other two pores are hydrophilic and can be filled with water molecules. The basic structure and pore properties of Cu_3BTC_2 were first reported by Williams et al.[16] For our work, the MOFs was synthesized and well characterized by following previously reported procedure.[14] XRD and BET analyses revealed high crystallinity and surface area (1091 m^2g^{-1}), which guarantees successful synthesis (see Supporting Information, Fig. S4† and pore analysis result). The synthesized Cu_3BTC_2 was saturated with water by vaporization, by which Cu_3BTC_2 containing 36 wt% of water was prepared and used during the entire experiment (Fig. S5†). The complete water-filling of the hydrophilic Cu_3BTC_2 pores blocks gas inclusion and physically causes a significant reduction in active storage sites for gas molecules in hydrophilic pores and makes the remaining pores to be available for the inclusion of target molecules.

From here, we report the results from our attempt to demonstrate the potential of HPB for separating CH_4 from a gaseous CH_4/N_2 mixture with remarkably high selectivity. Fig. 1A represents the amount of captured CH_4 and N_2 per 1 g of hydrophilic pore-blocked Cu_3BTC_2 (HPB-Cu_3BTC_2), according to system pressure. The amount of CH_4 stored in the MOF matrix increased rapidly to 50 bar, but at higher pressures, the rate of increase slowed and reached 1.5 $mmolg^{-1}$ at 100 bar. In contrast, the stored N_2 showed a slight tendency to increase with 0.13 $mmolg^{-1}$ at 100 bar. Consider that the CH_4 stored in dried Cu_3BTC_2 is reported to be 11.6 $mmolg^{-1}$.[17] Of course, the water-filling of the hydrophilic pores leads to considerable reduction of total stored CH_4 as the water-filling completely blocks occupation by gaseous molecules in large pores. The overall scheme of competitive CH_4 selection versus N_2 rejection is depicted in Fig. 1B. We analyzed the composition of the gas captured in HPB-Cu_3BTC_2 after direct exposure to an equimolar mixture of CH_4/N_2. Fig. 1C shows the separation performance of HPB-Cu_3BTC_2 with applied pressure at -30 ℃ (see Table S1 for specific data), by which CH_4 was enriched up to 95.8 mol% from a 50 mol% feed stream with the equilibrium selectivity of 24.7 at 80 bar, calculated from $(Y_{CH4}/Y_{N2}) \times (X_{N2}/X_{CH4})$, where X and Y indicate the mol fractions of each gas in the gaseous and material phases at equilibrium, respectively. In addition the CH_4/N_2 (90/10) feed stream can be enriched to more than 99 % CH_4. The highest equilibrium selectivity of HPB-Cu_3BTC_2 is much higher than both experimental (about 3, Fig. S6†) and simulation results (about 4) of Cu_3BTC_2 itself.[18] In addition we would like to point out that the storage and separation test was performed at -30 ℃ to prevent the emission of stored gas from solid phase and perform precise analysis. It is noteworthy to perform analysis at wide temperature and pressure range in the future.

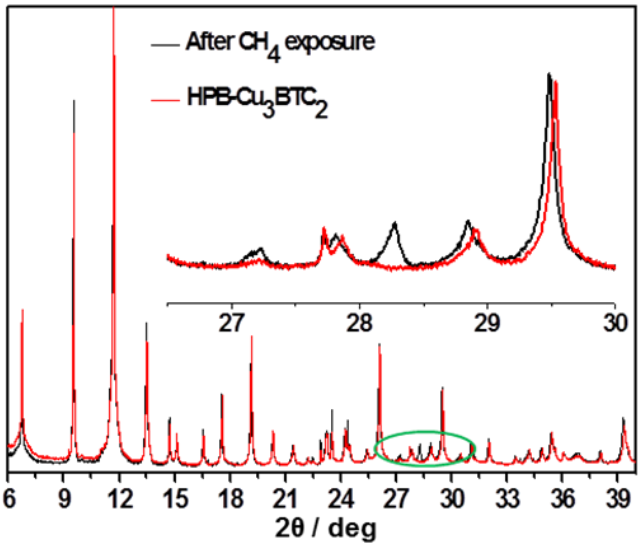

Fig. 2 High resolution powder diffraction (HRPD) of HPB-Cu_3BTC_2 (red) and CH_4 -included HPB-Cu_3BTC_2 (black) at 100 bar. The subset is the enlarged view of the circled region. Two new peaks are indexed to CH_4 hydrate.

To elucidate the origin of CH_4 storage and high selectivity of this method, we first conducted structural analysis by high-resolution powder diffraction with synchrotron radiation at the Pohang Accelerator Laboratory. The diffraction results for HPB-Cu_3BTC_2 before and after CH_4 exposure at 100 bar are shown in Fig. 2. A few new peaks were detected and merged at 27.2 ° and 28.3 ° corresponding to (320) and (321) diffractions of crystalline structure I CH_4 hydrate. Only a small fraction of the water in mesopores and on the Cu_3BTC_2 surface is likely to combine with CH_4 and formed stable methane hydrate. The CH_4 inclusions in Cu_3BTC_2 caused lattice expansion, but there was no notable change in peak intensities. The lattice parameter of Cu_3BTC_2 calculated from the (222) peak of highest intensity, increased from 26.3314 Å to 26.3651 Å, providing more stable confined spaces for capturing guest molecules.

The HPB-Cu_3BTC_2 samples pressurized at 100 bar of CH_4 were analyzed using Raman and 13C CP-MAS Solid NMR and the results are shown in Fig. 3A and 3B. In these, the Raman spectra were collected at -180 ℃ and ambient pressure. Three peaks corresponding to C-H symmetry stretching vibrational mode of CH_4 were observed at 2896.8, 2902.8 and 2913.8 cm^{-1}, which correspond to shifts by -20.2, -14.2 and -3.2 cm^{-1} from free CH_4 molecules. The last two peaks belong to CH_4 captured in structure I CH_4 hydrate. These peaks exhibited wavenumber deviations of -1 to about 2 from that of bulk gas hydrate. This resulted from the effect of Cu_3BTC_2 on neighbouring sI CH_4 hydrate. Excluding the possible influence of the appearance of a new hydrate phase, the highest peak was confirmed to result from CH_4 inclusion in the HPB-Cu_3BTC_2 framework. Earlier Raman analysis of CH_4 adsorption onto various MOFs indicated that the higher shift is caused by stronger interaction of CH_4 with the MOFs. The shift of -20.2 from HPB-Cu_3BTC_2 experiments is much higher than 7.6-10.1 cm^{-1} of IRMOFs.[19] The NMR spectrum in Fig. 3B shows four peaks at -4.3, -6.7, -11.2 and -12.7 ppm, where a chemical shift at -11.2 represents gaseous CH_4 weakly dissociated during measurements. That CH_4 itself might experience three distinctive inclusion states, which was also revealed by the Raman spectra.

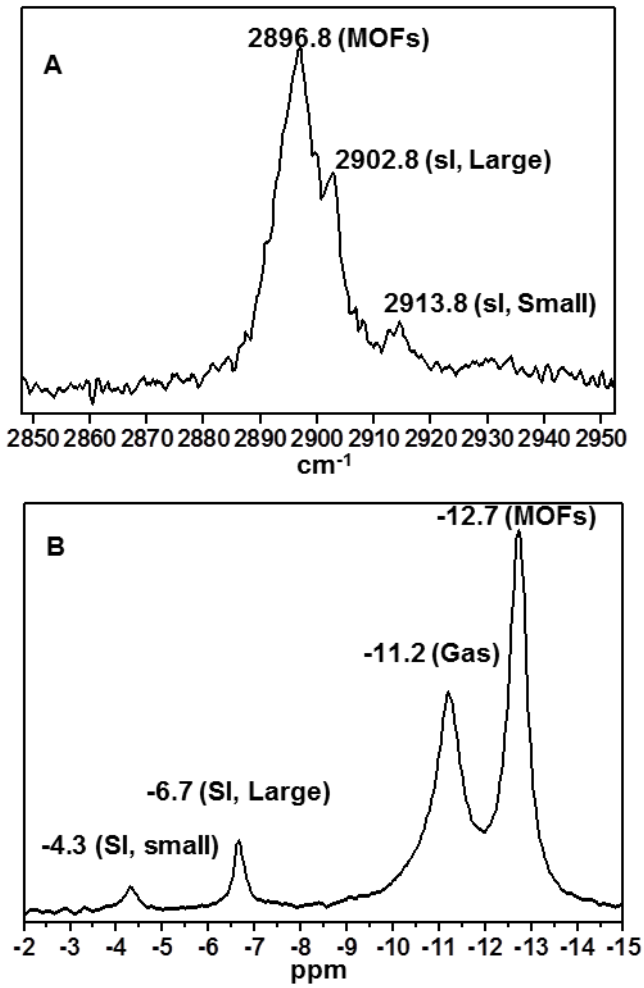

Fig. 3 Spectroscopic observations of CH_4 inclusion phenomena. (A) Raman and (B) 13C NMR spectra of CH_4 captured in HPB-Cu_3BTC_2.

The de-shielded small peaks at -4.3 and -6.7 ppm were assigned to CH_4 in small and large cages of sI CH_4 hydrate, respectively.[20]

The carbon nucleus of the CH_4 molecule included in the HPB-Cu_3BTC_2 resulted in the up-field shift of -11.2 to -12.7 ppm. It is known that the interaction between C-H and Π of the benzene ring induces a strong shielding effect for the carbon of CH_4.[21] The CH_4 actively participates in forming two coexisting phases: hydrate and Cu_3BTC_2, among which the amount of CH_4 in Cu_3BTC_2 is much greater than that of hydrate. This was well confirmed by the Raman spectra. At this stage, the question arises as to how CH_4 molecules occupy small empty hydrophobic pores in HPB-Cu_3BTC_2. The directly vaporized water can readily access the large hydrophilic pores of two distinctive sizes (Fig. 4A and 4B), and this would not allow capture of both CH_4 and N_2. In contrast, small pores surrounded by four benzene rings (strongly hydrophobic) remain vacant as they strongly repel water; thus forming stable niches where CH_4 molecules can be stored.[22] Because there was no noticeable change of HRPD peak patterns, we can speculate that the inclusion of CH_4 does not disturb the ordering of the water confined in the pore, nor affect close interaction between guest methane and pore water. In addition, the sharp NMR peak also confirms inclusion of CH_4 in small hydrophobic pores as shown in Fig. 4C. The geometrical aspect of the hydrophobic pores causes the methane molecules to be securely positioned. This is because the benzene rings of the hydrophobic pore form a tetrahedral arrangement with respect to the center of pore. We conjecture that the interaction of the four (C-H)s with the surrounding four π electrons causes higher Raman shift and nuclear shielding observed in the NMR. For more direct verification, we prepared two Cu_3BTC_2 samples saturated with tetrahydrofuran (THF) and water. Here, THF was specially chosen because it has a polar functional group that is known to form structure II hydrate.[23] THF is not able to enter the small pores, but it was acceptable that it fit well into large pores with water. Cu_3BTC_2 was immersed in solutions of 1 and 10 mol% THF, followed by a filtering process to remove excess solution from the outside of the MOF crystal surface. Then it was exposed to 100 bar of CH_4. As-prepared samples were analyzed by Raman spectroscopy, and the results are given in Fig. S7†. THF inclusion slightly shifts the CH_4 wavenumber to higher frequency, but there was no change in the peak intensity. This confirmed that the storage of CH_4 molecules in the hydrophobic pores was not affected by neighbouring THF molecules in hydrophilic pores.

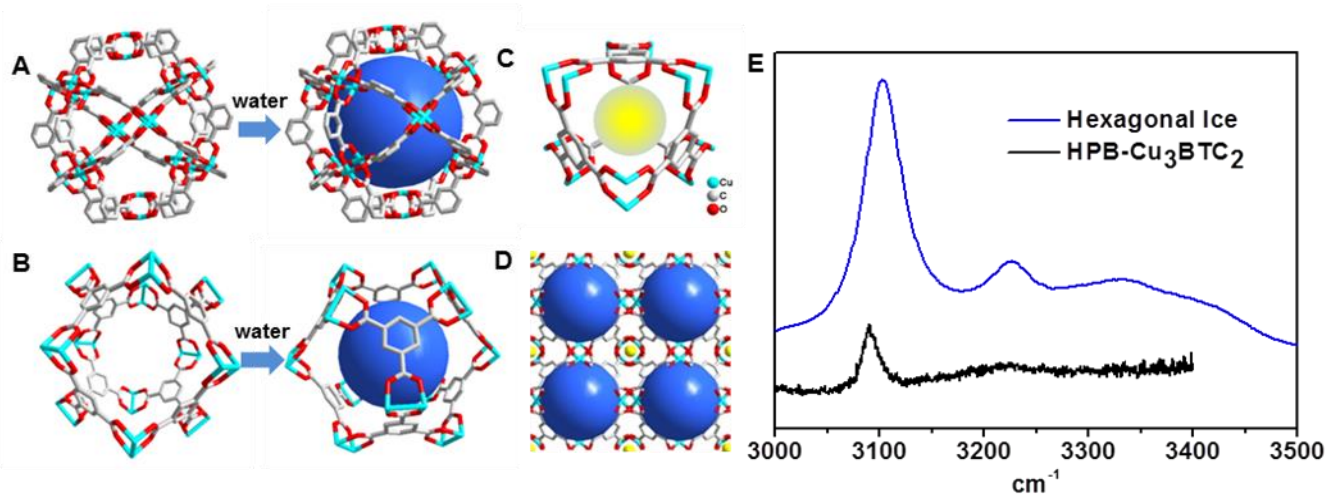

Fig. 4 Structural changes of Cu_3BTC_2. (A) and (B) Two distinctive hydrophilic large pores before and after water saturation. (C) Hydrophobic small pore after CH_4 inclusion. Yellow and blue spheres represent CH_4 molecules and water clusters, respectively. (D) Lattice structure of both CH_4 and water included Cu_3BTC_2. (E) Raman spectra of water in hexagonal ice phase (blue) and in HPB-Cu_3BTC_2 (black).

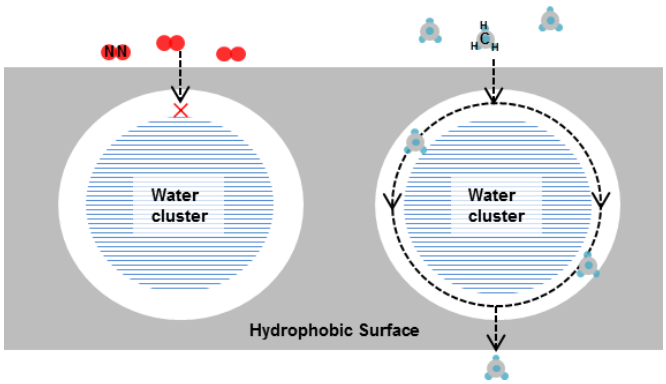

Fig. 5 Schematic description of the diffusion of N_2 (left) and CH_4 (right) in water-filled pore of Cu_3BTC_2, respectively.

In addition to the stronger interaction of hydrophobic pore with CH_4 over N_2, the water confined in Cu_3BTC_2 also contributes to higher methane selectivity by inducing more favour environment for diffusion of CH_4 over N_2. It is known that the confining environment provides favorable condition for the formation of hydrogen bonded water clusters, which structure is like solid ice and can be stable even at room temperature.[24-28] This kind of hydrogen bonded water structure can be formed in the hydrophilic pore of Cu_3BTC_2. To verify how the confined water molecules exist in the pores of Cu_3BTC_2, we performed Raman analysis on the OH-stretching vibration of water, which provides information about its dynamics. In general, liquid water shows a broad O-H stretching peak from 3100-3600 cm^{-1} due to the overtone of four different vibration modes (I to IV).[29] As water transforms to solid phase at low temperature or become confined in nano-sized space, a sharp peak corresponding to mode V appears (~3100 cm^{-1}), which indicates formation of tetrahedral hydrogen bonding between molecules.[30-33] For this reason the Mode-V peak is an induicator of solid water phase. In Fig. 4E the water confined in Cu_3BTC_2 shows high sharp V-peak at room temperature, which confirms that the water is fixed and ordered by hydrogen bonding even at room temperature. This strongly blocks the hydrophilic pores of MOFs. To cross-check this interpretation we used Differential Scanning Calorimetry (DSC) for HPB-Cu_3BTC_2 (Fig. S8†). During a cooling and heating cycle from 20 to -40 ℃, the first-order structure transition of water to solid ice was not observed.

At the circumstance that the pore is filled with water, two pathways can be expected for the gas diffusion in to the material. One is gas diffusion through confined water and the other one is through the interface between hydrophobic surface of MOFs and confined water. Considering that the diffusion coefficient of gas in tetrahedrally ordered solid water phase is extremely smaller than liquid water, e. g., diffusion coefficient of CH_4 in hexagonal ice is 5 orders of magnitude less than that of liquid water,[34,35] gas diffusion through confined water is not significant. Furthermore the CH_4 and N_2 gas are not strongly interact with water. Therefore the interaction between hydrophobic surface and gas molecule is important factor for the storage and separation. As previous reports revealed, the effects of polarizability on the adsorption and separation of gas, the gas with higher polarizability can have stronger interaction with hydrophobic surface, vice versa.[36-39] In the case of separating CH_4/N_2, the polarizability of CH_4 and N_2 is 2.448 $Å^3$ and 1.710 $Å^3$, respectively.[3] CH_4 with higher polarizability have higher chance to interact with surface of MOFs and diffuse in to the HPB-Cu_3BTC_2 as shown in Fig. 5. The specific description about the pore structure of water-filled hydrophilic pore can be found elsewhere: small free voids exist between hydrophobic wall and water cluster due to bridging effect.[14]

To verify our mechanism for higher CH_4 selectivity than N_2, we observed the change of CH_4/N_2 selectivity of Cu_3BTC_2 in terms of water content in MOF in Fig. S9†. With the presence of water, the CH_4/N_2 selectivity increased slightly, however, significant high selectivity was achieved at enough high water content to block the hydrophilic pore of Cu_3BTC_2. This result confirms that our mechanism for higher CH_4 selectivity over N_2 is reasonable.

Additionally, we measured storage and dissociation kinetics as shown in Fig. 6. The initial pressure of 81 bar in the reactor containing HPB-Cu_3BTC_2 rapidly decreased to 77.4 bar within 10 min with high CH_4 absorption, and then slowly decreased to 76.5 bar.

Expulsion of CH_4 from the cage according to temperature change could be observed using XRD and Raman spectroscopy. The Raman peaks of CH_4 rapidly disappeared between -40 ℃ and -20 ℃ due to its dissociation as shown in Fig. 6B, and XRD showed a dramatic structural change between -60 and -40 ℃ due to the emission of gas and water from pores as shown in Fig. S10†. A slight deviation of dissociation temperatures is likely attributable to the difference in pressure during Raman spectroscopy (1 bar) and XRD (vacuum). We observed that 80 % of stored CH_4 was rapidly dissociated within 5 min, but that additional heating was needed for complete recovery (Fig. 6C).

To check the stability of Cu_3BTC_2 in our working condition, we observed separation capability during 10 times of repeating test over 5 days, which showed maintenance of separation performance (Fig. S11†). After that, we recovered HPB-Cu_3BTC_2 and performed XRD measurement, which showed sharp diffraction peaks (Fig. S12†) and confirmed the maintenance of structure during gas separation. Also, the mass of HPB-Cu_3BTC_2 after exposure to 10 times of dry CH_4/N_2 mixture is not changed, which means the water confined in Cu_3BTC_2 is not removed in our working condition, even after 10 times of contacts with dry gas.

Considering the features of HPB-Cu_3BTC_2 such as 1) strong dependency of CH_4 storage capacity on pressure, 2) small storage

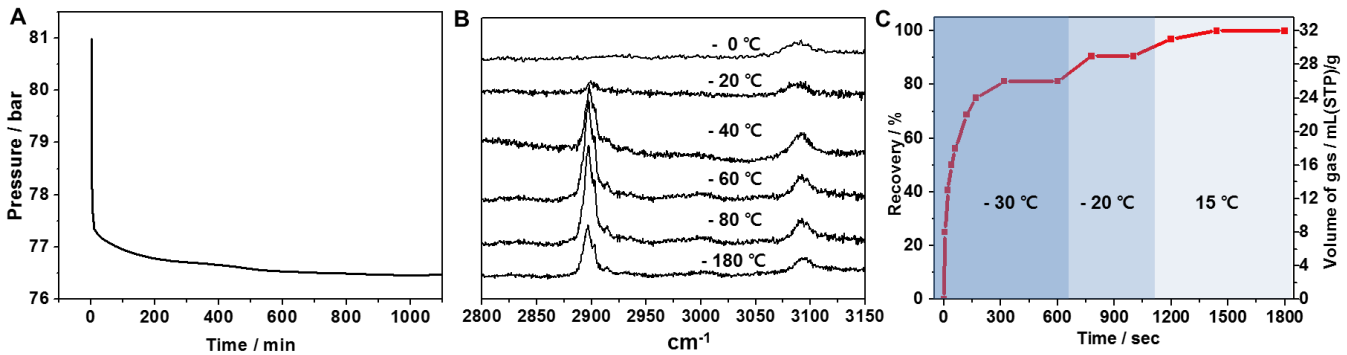

Fig. 6 (A) Adsorption and rate of CH_4 in HPB-Cu_3BTC_2 at -30 ℃. (B) Raman spectra of CH_4-included HPB-Cu_3BTC_2 at ambient pressure with increasing temperature. (C) Dissociation rate of stored CH_4.

capacity of N_2, and 3) recovery of stored gas and regeneration of material by just depressurization, this material could be used for pressure swing adsorption. Even though additional heating is required for complete recovery of adsorbed CH_4, the energy consumed for additional temperature swing could reduce the efficiency of this technology.

Despite of beneficial features of this method, additional researches should be followed in the near future for the actual use in natural gas fields, e.g. sensitivities toward other gases such as H_2S and CO_2 existing in natural gases.

Conclusions

The present outcomes clearly demonstrate that the extraordinary selectivity for CH_4 over N_2 is achieved by simple water saturation of Cu_3BTC_2. Furthermore, the methane gas can readily be recovered by pressurizing and depressurizing cycles (e.g., common pressure swing adsorption), leading to applications for natural gas processing, methane production from landfill gas and N_2 removal. Moreover, the ability to switch from hydrophilic to hydrophobic pores by selection of the most suitable guest filler is expected to facilitate extension of HPB to include the chemical fields of zeolites, other MOFs and silica materials. Also, formation of methane hydrate in the mesopore of Cu_3BTC_2 suggests the possible approach to combine MOF and gas hydrate technologies to develop enhanced gas storage and separation method. These new options should lead to further opportunities for the application of porous materials on gas separation.

Acknowledgements

This work was supported by National Research Foundation of Korea (NRF Grant No. 2010-0029176) funded by the Korea government (MSIP) and by the WCU program (R-31-10055-0). We gratefully acknowledge the Pohang Accelerator Laboratory (Beamline 9B-HRPD) and the Korea Basic Science Institute for use of the solid-state NMR.

References

1 J. D. Figueroa, T. Fout, S. Plasynski, H. McIlvried, R. D. Srivastava, *Int. J. Greenhouse Gas Control,* 2008, **2**, 9-20.
2 D. M. D'Alessandro, B. Smit, J. R. Long, *Angew. Chem. Inter. Ed.,* 2010, **49**, 6058-6082.
3 T. E. Rufford, S. Smart, G. C. Y. Watson, B. F. Graham, J. Boxall, J. C. D. da Costa, E. F. May, *J. Pet. Sci. Eng.,* 2012, **94-95**, 123-154.
4 H. W. Kim, H. W. Yoon, S. M. Yoon, B. M. Yoo, B. K. Ahn, Y. H. Cho, H. J. Shin, H. Yang, U. Paik, S. Kwon, J. Y. Choi, H. B. Park, *Science,* 2013, **342**, 91-95.
5 H. Li, Z. N. Song, X. J. Zhang, Y. Huang, S. G. Li, Y. T. Mao, H. J. Ploehn, Y. Bao, M. Yu, *Science,* 2013, **342**, 95-98.
6 E. D. Bloch, W. L. Queen, R. Krishna, J. M. Zadrozny, C. M. Brown, J. R. Long, *Science,* 2012, **335**, 1606-1610.
7 Z. R. Herm, B. M. Wiers, J. A. Mason, J. M. van Baten, M. R. Hudson, P. Zajdel, C. M. Brown, N. Masciocchi, R. Krishna, J. R. Long, *Science,* 2013, **340**, 960-964.
8 D. Britt, H. Furukawa, B. Wang, T. G. Glover, O. M. Yaghi, *Proc. Natl. Acad. Sci. USA,* 2009, **106**, 20637-20640.
9 A. Mallick, S. Saha, P. Pachfule, S. Roy, R. Banerjee, *J. Mater. Chem.,* 2010, **20**, 9073-9080.
10 S. Couck, J. F. M. Denayer, G. V. Baron, T. Remy, J. Gascon, F. Kapteijn, *J. Am. Chem. Soc.,* 2009, **131**, 6326–6327.
11 A. Torrisi, R. G. Bell, C. Mellot-Draznieks, *Cryst. Growth. Des.,* 2010, **10**, 2839-2841.
12 M. Wriedt, J. P. Sculley, A. A. Yakovenko, Y. G. Ma, G. J. Halder, P. B. Balbuena, H. C. Zhou, *Angew. Chem. Inter. Edi.,* 2012, **51**, 9804-9808.
13 J. R. Li, J. M. Yu, W. G. Lu, L. B. Sun, J. Sculley, P. B. Balbuena, H. C. Zhou, *Nat. Commun.,* 2013, **4**. DOI: 10.1038/ncomms2552.
14 P. Kusgens, M. Rose, I. Senkovska, H. Frode, A. Henschel, S. Siegle, S. Kaskel, *Microporous Mesoporous Mater.,* 2009, **120**, 325-330.
15 P. J. Ryan, O. K. Farha, L. J. Broadbelt, R. Q. Snurr, Y.-S. Bae, US Pat. 20120073438 A1, 2012.
16 S. S.-Y. Chui, S. M.-F. Lo, J. P. H. Charmant, A. G. Orpen, I. D. Williams, *Science,* 1999, **283**, 1148-1150.
17 I. Senkovska, S. Kaskel, *Microporous Mesoporous Mater.,* 2008, **112**, 108-115.
18 B. Liu, B. Smit, *Langmuir,* 2009, **25**, 5918-5926.
19 D. Y. Siberio-Pe´rez, A. G. Wong-Foy, O. M. Yaghi, A. J. Matzger, *Chem. Mater.,* 2007, **19**, 3681-3685.
20 E. D. Sloan, C. A. Koh (2008) in *Clathrate hydrates of natural gases Third Edition,*CRC Press, USA. pp.353.
21 J. A. Platts, K. Gkionis, *Phys. Chem. Chem. Phys.,* 2009, **11**, 10331-10339.
22 H. Wu, J. M. Simmons, Y. Liu, C. M. Brown, X. S. Wang, S. Ma, V. K. Peterson, P. D. Southon, C. J. Kepert, H. C. Zhou, T. Yildirim, W. Zhou, *Chem. Eur. J.,* 2010, **16**, 5205-5214.
23 L. J. Florusse, C. J. Peters, J. Schoonman, K. C. Hester, C. A. Koh, S. F. Dec, K. N. Marsh, E. D. Sloan, *Science,* 2004, **306**, 469-471.
24 M. L. Wei, C. He, W. J. Hua, C. Y. Duan, S. H. Li, Q. J. Meng, *J. Am. Chem. Soc.,* 2006, **128**, 13318-13319.
25 Y. Wang, T. A. Okamura, W. Y. Sun, N. Ueyama, *Cryst. Growth Des.* 2008, **8**, 802-804.
26 M. L. Cao, J. J. Wu, H. J. Mo, B. H. Ye, *J. Am. Chem. Soc.* 2009, **131**, 3458-3459.
27 C. M. Jin, Z. Zhu, Z. F. Chen, Y. J. Hu, X. G. Meng, *Cryst. Growth. Des.,* 2010, **10**, 2054-2056.
28 Z. Yang, S. G. Hua, W. J. Hua, S. H. Li, *J. Phys. Chem. B,* 2011, **115**, 8249-8256.
29 Q. Sun, *Vib. Spectrosc.* 2009, **51**, 213-217.
30 C. G. Venkatesh, S. A. Rice, J. B. Bates, *J. Chem. Phys.,* 1975, **63**, 1065-1071.
31 T. C. Sivakumar, S. A. Rice, M. G. Sceats, *J. Chem. Phys.,* 1978, **69**, 3468-3476.
32 F. Mallamace, M. Broccio, C. Corsaro, A. Faraone, D. Majolino, V. Venuti, L. Liu, C. Y. Mou, S. H. Chen, *Proc. Natl. Acad. Sci. USA,* 2007, **104**, 424-428.
33 M. Erko, G. H. Findenegg, N. Cade, A. G. Michette, O. Paris, *Phys. Rev. B,* 2011, **84**. 104205.
34 A. Hori, T. Hondoh, *Can. J. Phys.,* 2003, **81**, 251-259.
35 M. Takahata, Y. Kashiwaya, K. Ishii, *Mater. Trans.,* 2010, **51**, 727-734.
36 S. L. Suib, *Science,* 2003, **302**, 1335-1336.
37 S. T. Meek, S. L. Teich-McGoldrick, J. J. Perry, J. A. Greathouse, M. D. Allendorf, *J. Phys. Chem. C,* 2012, **116**, 19765-19772.
38 J. F. Yang, J. M. Li, W. Wang, L. B. Li, J. P. Li, *Ind. Eng. Chem. Res.,* 2013, **52**, 17856-17864.
39 P. S. Yaremov, N. D. Scherban, V. G. Ilyin, *Theor. Exp. Chem.,* 2013, **48**, 394-400.

